Acta Crystallographica Section C
**Crystal Structure Communications**
ISSN 0108-2701

# Two modes of O—H···O hydrogen bonding utilized in dimorphs of racemic 6-*O*-acryloyl-2-*O*-benzoyl-*myo*-inositol 1,3,5-orthoformate

**Shobhana Krishnaswamy,[a]* Rajesh G. Gonnade,[a] Mohan M. Bhadbhade[b] and Mysore S. Shashidhar[c]**

[a]Centre for Materials Characterization, National Chemical Laboratory, Pune 411 008, India, [b]Analytical Centre, University of New South Wales, Sydney, Australia, and [c]Division of Organic Chemistry, National Chemical Laboratory, Pune 411 008, India
Correspondence e-mail: s.krishnaswamy@ncl.res.in

Received 21 November 2008
Accepted 5 January 2009
Online 10 January 2009

The title compound, $C_{17}H_{16}O_8$, yields conformational dimorphs [forms (I) and (II)] at room temperature, separately or concomitantly, depending on the solvent of crystallization. The yield of crystals of form (I) is always much more than that of crystals of form (II). The molecule has one donor –OH group that can make intermolecular O—H···O hydrogen bonds with one of the two acceptor C=O groups, as well as with the hydroxyl O atom; interestingly, each of the options is utilized separately in the dimorphs. The crystal structure of form (I) contains one molecule in the asymmetric unit and is organized as a planar sheet of centrosymmetric dimers *via* O—H···O hydrogen bonds involving the OH group and the carbonyl O atom of the acryloyl group. In the crystal structure of form (II), which contains two independent molecules in the asymmetric unit, two different O—H···O hydrogen bonds, *viz*. hydroxyl–hydroxyl and hydroxyl–carbonyl (benzoyl), connect the molecules in a layered arrangement. Another notable feature is the transformation of form (II) to form (I) *via* melt crystallization upon heating to 411 K. The higher yield of form (I) during crystallization and the thermal transition of form (II) to form (I) suggest that the association in form (I) is more highly favoured than that in form (II), which is valuable in understanding the priorities of molecular aggregation during nucleation of various polymorphs.

## Comment

*myo*-Inositol 1,3,5-orthoester derivatives serve as key intermediates (Sureshan *et al.*, 2003) for the preparation of biologically relevant *myo*-inositol phosphates, which play a significant role in cellular signal transduction pathways (Potter & Lampe, 1995). The title compound, (1), was synthesized to examine the acyl transfer reactivities in crystals of *myo*-inositol orthoester derivatives carrying different ester groups (Praveen *et al.*, 1998; Sarmah *et al.*, 2005; Murali *et al.*, 2007). We report here the structures of dimorphs of (1), namely form (I) (plates) and form (II) (needles). The two sets of atom numbers for the C atoms of the inositol ring in the scheme below refer to the two enantiomers: anticlockwise numbering for the D configuration and clockwise numbering for the L configuration (Parthasarathy & Eisenberg, 1986).

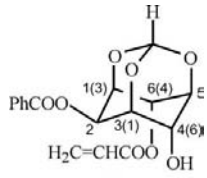


(1)

Single-crystal X-ray intensity measurements for crystals of form (I) were recorded at ambient temperature (297 K), while data for crystals of form (II) were measured at 133 K to minimize the large thermal anisotropies observed for the phenyl ring atoms at room temperature. Crystals of racemic form (I) are triclinic, space group $P\overline{1}$ (Fig. 1), while racemic form (II) crystallizes in the noncentrosymmetric space group $P2_1$, with two independent molecules (*A* and *B*) in the asymmetric unit being an enantiomorphic pair (Fig. 2). The two molecules in the crystal structure of form (II) show significant differences in the torsion angles associated with the three functional groups, namely C1—C2—O2—C8 (the benzoyl group), C1—C6—O6—C15 (the acryloyl group) and C3—C4—O4—H18 (the hydroxyl group). The torsion-angle difference for the benzoyl group is 20°, for the acryloyl group is 15° and for the hydroxyl group is 34° (Table 3). The molecular overlap of form (I) and molecule *A* of form (II) reveals major conformational changes in the hydroxyl groups and in the benzoyl groups (Fig. 3, and Tables 1 and 3). The orientations of the hydroxyl groups are almost reversed (113°), whereas the benzoyl groups show a difference of ∼52° in their torsion angles. The difference in the torsion angles of the acryloyl group (C1—C6—O6—C15) is 13°. These conformational changes in the three functional groups have a profound influence on the molecular association in the dimorphs.

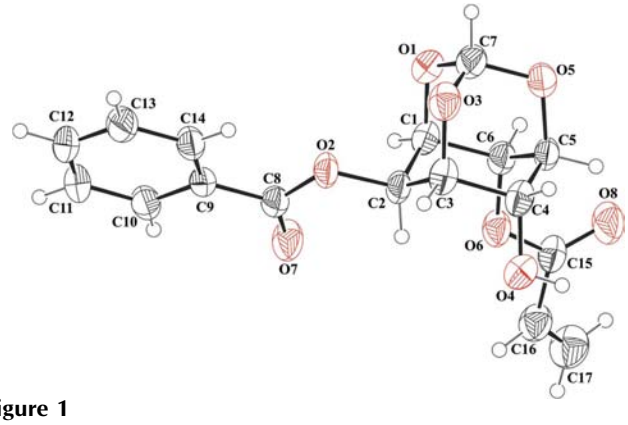


**Figure 1**
The molecular structure of form (I) of (1) [the (1*S*,3*R*,5*S*)-enantiomer], showing the atom-labelling scheme. Displacement ellipsoids are drawn at the 40% probability level and H atoms are shown as small spheres of arbitrary radii.

  doi:10.1107/S0108270109000225 

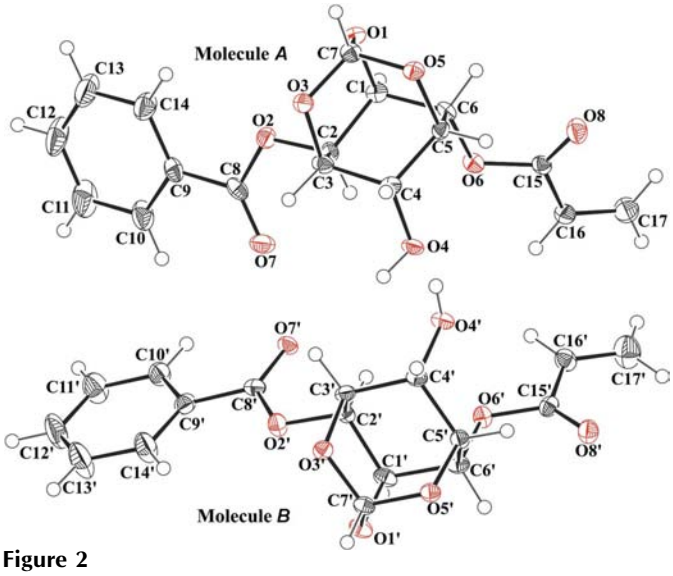


**Figure 2**
The molecular structure of form (II) of (1) [the reference coordinates defined for molecules *A* and *B* have (1*S*,3*R*,5*S*) and (1*R*,3*S*,5*R*) configurations, respectively], showing the atom-labelling scheme. Displacement ellipsoids are drawn at the 40% probability level and H atoms are shown as small spheres of arbitrary radii.

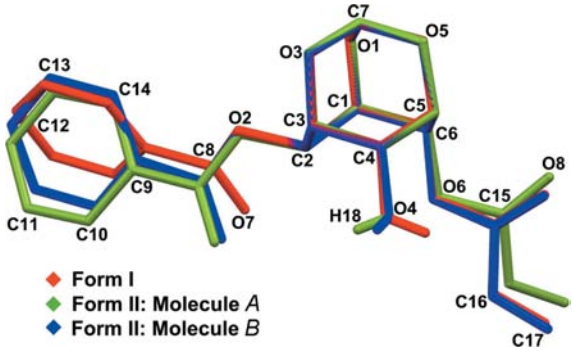


**Figure 3**
Overlap diagram of molecules in forms (I) and (II).

The hydroxyl group forms different intermolecular O—H···O hydrogen bonds in the crystal structures of forms (I) and (II). In form (I), adjacent molecules form centrosymmetric dimers *via* O—H···O hydrogen bonds involving the OH group (O4—H18) and acryloyl carbonyl atom O8 (Fig. 4 and Table 2). In form (II), the –OH groups of the two symmetry-independent molecules are involved in a hydrogen-bonding interaction (O4′—H18′···O4). The acceptor atom O4 also acts as a donor in a hydroxyl–carbonyl interaction (O4—H18···O7$^{i}$; see Table 4 for all symmetry codes), resulting in a catemeric arrangement along the *c* axis (Fig. 5). Additionally, five supporting C—H···O interactions (C1—H1···O5$^{ii}$, C1′—H1′···O5′$^{ii}$, C3—H3···O7$^{i}$, C3′—H3′···O7 and C16—H16···O4′) hold the molecules within the chain.

The hydrogen-bonded units thus formed make different three-dimensional patterns of molecular organization in the polymorphs. In form (I), O—H···O-linked centrosymmetric dimers form a planar structure. In form (II), each molecule in the asymmetric unit forms a dimer by aggregating sideways, bringing orthoformate groups closer *via* noncentrosymmetric

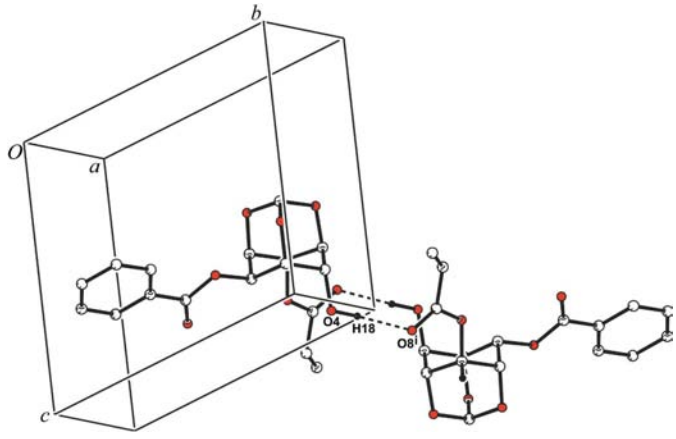


**Figure 4**
The dimer formed by O—H···O hydrogen bonding in form (I). For the sake of clarity, H atoms not involved in hydrogen bonding have been omitted. [Symmetry code: (i) $-x+2, -y+2, -z+2$.]

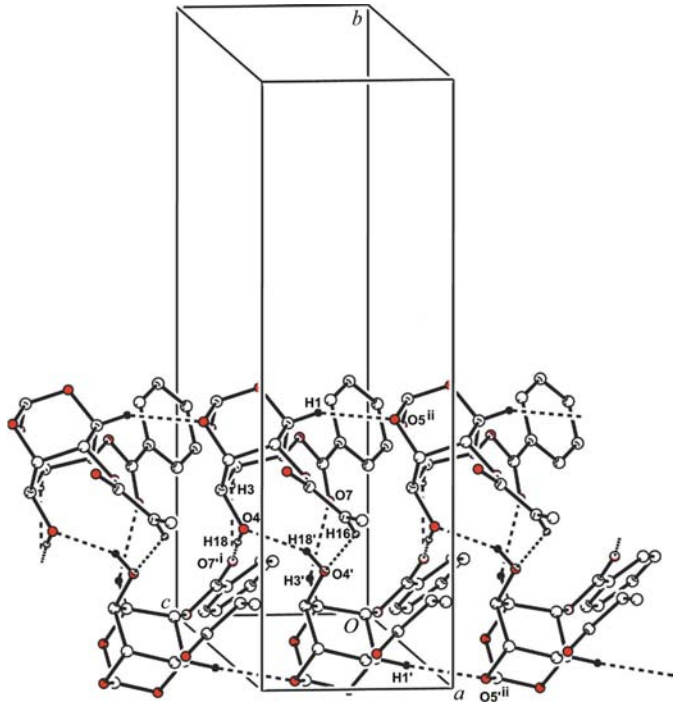


**Figure 5**
Molecules linked *via* two different O—H···O hydrogen bonds and other weak C—H···O interactions in form (II), leading to a catemeric arrangement running parallel to the *c* axis. For the sake of clarity, H atoms not involved in hydrogen bonding have been omitted. [Symmetry codes: (i) $x, y, z+1$; (ii) $x, y, z-1$.]

C—H···O interactions (C7—H7···O8′$^{iii}$, C6—H6···O5′$^{iii}$ and C7′—H7′···O8$^{iv}$) of comparable strength (Table 4). These dimeric units are are further joined *via* O4′—H18′···O4, C3′—H3′···O7 and C16—H16···O4′ hydrogen-bonding interactions, thus forming a chain extending along the *b* axis. Neighbouring chains are weakly associated along the *a* axis *via* C12′—H12′···O8′$^{v}$ and C13—H13···O3′$^{vi}$ contacts, thus forming a layered arrangement (Fig. 6).

A differential scanning calorimetry study of crystals of form (I) shows only a single endotherm at 426 K, while crystals of

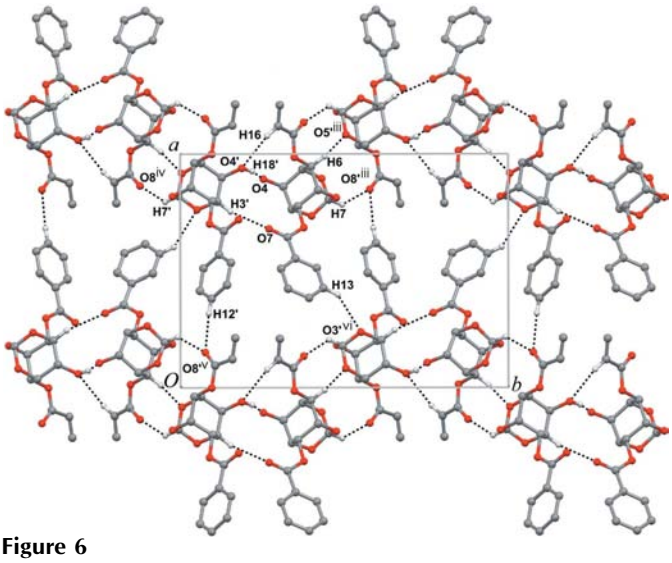


**Figure 6**
The packing of molecules in the crystal structure of form (II). Dashed lines indicate intermolecular C—H···O and O—H···O interactions. For the sake of clarity, H atoms not involved in hydrogen bonding have been omitted. [Symmetry codes: (iii) $-x+2, y+\frac{1}{2}, -z+2$; (iv) $-x+2, y-\frac{1}{2}, -z+2$; (v) $x-1, y, z-1$; (vi) $-x+1, y+\frac{1}{2}, -z+1$.]

form (II) show two endothermic peaks. The first of these, at 411 K, was established by hot-stage microscopy to be the structural phase transition to form (I) *via* a molten phase. The second endotherm at 425 K corresponds to the melting of the crystals of form (I). While single-crystal to single-crystal thermal phase transitions have been reported earlier in *myo*-inositol derivatives (Steiner *et al.*, 1993; Gonnade *et al.*, 2005, 2008), in this instance the conversion of form (II) to form (I) occurs *via* melt crystallization, often observed amongst polymorphs of pharmaceutical crystals (Cosgrove *et al.*, 2005; Wishkerman & Bernstein, 2006; Vega *et al.*, 2006; Roy *et al.*, 2007; Grooff *et al.*, 2007). Thus, form (II) upon heating transforms irreversibly to form (I).

In conclusion, orientational changes in a small functional group like –OH (Ibberson *et al.*, 2008) and the benzoyl group induce diverse hydrogen-bonding patterns in molecular associations and result in polymorphic modifications. The significantly higher yield of form (I) over form (II), and the irreversible transformation of form (II) to form (I), suggest a preference for a dimeric O—H···O hydrogen bond over a catemeric O—H···O hydrogen bond (Das & Desiraju, 2006) in nucleation and crystal growth.

## Experimental

For the preparation of (1), freshly prepared acryloyl chloride (0.182 g, 2 mmol) was added to a cooled solution of 2-*O*-benzoyl-*myo*-inositol 1,3,5-orthoformate (0.588 g, 2 mmol; Samanta *et al.*, 1998) and dry triethylamine (0.405 g, 6 mmol) in dry dimethylfomamide (DMF, 12 ml) and the reaction mixture was stirred at room temperature for 12 h. The DMF was evaporated under reduced pressure, and the residue was diluted with dichloromethane and washed with water, dilute HCl, saturated sodium bicarbonate solution and brine. The organic layer was dried with anhydrous sodium sulfate and concentrated, and the product purified by column chromatography to obtain (1) (yield 0.25 g, 36%). IR $\lambda_{max}$ (Nujol, cm$^{-1}$): 1728, 1701, 3444; $^1$H NMR (200 MHz, $CDCl_3$, $Me_4Si$): $\delta$ 2.56–2.59 (1H, $J$ = 6.1 Hz, *d*, OH), 4.43–4.49 (1H, *m*, Ins H), 4.50–4.57 (2H, *m*, Ins H), 4.63–4.74 (1H, *m*, Ins H), 5.52–5.55 (1H, $J$ = 1.6 Hz, *q*, Ins H), 5.62 (1H, $J$ = 1.3 Hz, *d*, Ins H), 5.66–5.71 (1H, $J$ = 3.9 and 1.6 Hz, *td*, CH), 5.93–6.56 (3H, *m*, CH═$CH_2$), 7.43–7.65 (3H, *m*, ArH), 8.13–8.19 (2H, *m*, Ar H); $^{13}$C NMR (125 MHz, $CDCl_3$): $\delta$ 63.3 (Ins C), 67.2 (Ins C), 68.1 (Ins C), 69.2 (Ins C), 71.5 (Ins C), 102.6 ($O_3C$), 126.9 (Ar C), 128.2 (Ar C, s), 129.2 (Ar C), 129.7 (Ar C, s), 132.7 ($CH_2$), 133.3 (═CH), 164.2 (C═O), 166 (C═O).

Crystallization of (1) from ethyl acetate (containing only a trace of light petroleum) and from other common solvents (dichloromethane, toluene, methanol, tetrahydrofuran, chloroform and benzene) yielded exclusively plates [form (I), m.p. 421–423 K], whereas crystallization from an ethyl acetate–light petroleum mixture (1:1 *v*/*v*) produced needle-shaped crystals [form (II), m.p. 410–412 K]. Crystallization from a dichloromethane–light petroleum mixture yielded both forms concomitantly; the relative yield of crystals of form (II) was always much less than that of crystals of form (I). All the crystallization experiments were carried out under comparable conditions.

### Form (I) of compound (1)

*Crystal data*

$C_{17}H_{16}O_8$
$M_r$ = 348.30
Triclinic, $P\overline{1}$
$a$ = 8.8808 (6) Å
$b$ = 9.5502 (6) Å
$c$ = 9.7100 (6) Å
$\alpha$ = 102.2660 (10)°
$\beta$ = 101.7330 (10)°
$\gamma$ = 94.3340 (10)°
$V$ = 781.83 (9) Å$^3$
$Z$ = 2
Mo $K\alpha$ radiation
$\mu$ = 0.12 mm$^{-1}$
$T$ = 297 (2) K
0.56 × 0.43 × 0.19 mm

*Data collection*

Bruker SMART APEX CCD area-detector diffractometer
Absorption correction: multi-scan (*SADABS*; Bruker, 2003)
$T_{min}$ = 0.936, $T_{max}$ = 0.978
9163 measured reflections
2755 independent reflections
2374 reflections with $I > 2\sigma(I)$
$R_{int}$ = 0.014

**Table 1**
Selected torsion angles (°) for form (I) of (1).

| | | | |
|---|---|---|---|
| C8—O2—C2—C1 | 87.3 (2) | C3—C4—O4—H18 | −172 (3) |
| C15—O6—C6—C1 | 166.90 (18) | | |

**Table 2**
Hydrogen-bond geometry (Å, °) for form (I) of (1).

| *D*—H···*A* | *D*—H | H···*A* | *D*···*A* | *D*—H···*A* |
|---|---|---|---|---|
| O4—H18···O8$^{i}$ | 0.95 (5) | 1.98 (5) | 2.930 (3) | 174 (4) |

Symmetry code: (i) $-x+2, -y+2, -z+2$.

**Table 3**
Selected torsion angles (°) for form (II) of (1).

| | | | |
|---|---|---|---|
| C1—C2—O2—C8 | 139.0 (4) | C1′—C6′—O6′—C15′ | −168.4 (3) |
| C1—C6—O6—C15 | 153.8 (3) | C3—C4—O4—H18 | −59 (3) |
| C1′—C2′—O2′—C8′ | −119.5 (4) | C3′—C4′—O4′—H18′ | 93 (4) |

**Table 4**
Hydrogen-bond geometry (Å, °) for form (II) of (1).

| $D$—H···$A$ | $D$—H | H···$A$ | $D$···$A$ | $D$—H···$A$ |
|---|---|---|---|---|
| O4′—H18′···O4 | 0.84 (6) | 2.09 (6) | 2.858 (5) | 151 (5) |
| O4—H18···O7′$^{i}$ | 0.82 (5) | 1.98 (5) | 2.785 (4) | 165 (4) |
| C1—H1···O5$^{ii}$ | 1.00 | 2.43 | 3.364 (5) | 155 |
| C1′—H1′···O5′$^{ii}$ | 1.00 | 2.59 | 3.533 (5) | 157 |
| C3—H3···O7′$^{i}$ | 1.00 | 2.39 | 3.161 (5) | 133 |
| C3′—H3′···O7 | 1.00 | 2.58 | 3.482 (5) | 150 |
| C16—H16···O4′ | 0.95 | 2.55 | 3.308 (5) | 136 |
| C7—H7···O8′$^{iii}$ | 1.00 | 2.50 | 3.328 (5) | 140 |
| C6—H6···O5′$^{iii}$ | 1.00 | 2.39 | 3.208 (5) | 138 |
| C7′—H7′···O8$^{iv}$ | 1.00 | 2.43 | 3.202 (5) | 133 |
| C12′—H12′···O8′$^{v}$ | 0.95 | 2.60 | 3.540 (6) | 171 |
| C13—H13···O3′$^{vi}$ | 0.95 | 2.59 | 3.416 (6) | 145 |

Symmetry codes: (i) $x, y, z+1$; (ii) $x, y, z-1$; (iii) $-x+2, y+\frac{1}{2}, -z+2$; (iv) $-x+2, y-\frac{1}{2}, -z+2$; (v) $x-1, y, z-1$; (vi) $-x+1, y+\frac{1}{2}, -z+1$.

*Refinement*

$R[F^2 > 2\sigma(F^2)] = 0.053$
$wR(F^2) = 0.152$
$S = 1.04$
2755 reflections
230 parameters
H atoms treated by a mixture of independent and constrained refinement
$\Delta\rho_{max} = 0.44$ e Å$^{-3}$
$\Delta\rho_{min} = -0.14$ e Å$^{-3}$

### Form (II) of compound (1)

*Crystal data*

$C_{17}H_{16}O_8$
$M_r = 348.30$
Monoclinic, $P2_1$
$a = 13.813$ (4) Å
$b = 19.279$ (5) Å
$c = 5.9801$ (15) Å
$\beta = 96.665$ (4)°
$V = 1581.8$ (7) Å$^3$
$Z = 4$
Mo $K\alpha$ radiation
$\mu = 0.12$ mm$^{-1}$
$T = 133$ (2) K
0.19 × 0.12 × 0.05 mm

*Data collection*

Bruker SMART APEX CCD area-detector diffractometer
Absorption correction: multi-scan (*SADABS*; Bruker, 2003)
$T_{min} = 0.978$, $T_{max} = 0.994$
15127 measured reflections
2870 independent reflections
2669 reflections with $I > 2\sigma(I)$
$R_{int} = 0.075$

*Refinement*

$R[F^2 > 2\sigma(F^2)] = 0.048$
$wR(F^2) = 0.114$
$S = 1.14$
2870 reflections
459 parameters
1 restraint
H atoms treated by a mixture of independent and constrained refinement
$\Delta\rho_{max} = 0.29$ e Å$^{-3}$
$\Delta\rho_{min} = -0.20$ e Å$^{-3}$

All H atoms (except hydroxyl H atoms) were placed in geometrically idealized positions for both forms. For form (I), C—H = 0.98 Å for the inositol ring H atoms and orthoformate H atom, and C—H = 0.93 Å for the aromatic and alkenyl H atoms. For form (II), C—H = 1.00 Å for the inositol ring H atoms and orthoformate H atom, and C—H = 0.95 Å for the aromatic and alkenyl H atoms. They were constrained to ride on their parent atoms, with $U_{iso}$(H) = $1.2U_{eq}$(C). The O-bound H atoms in both forms were located in difference Fourier maps and refined isotropically. The refined O—H distances were 0.95 (5) Å for form (I), and 0.82 (5) and 0.84 (6) Å for molecules *A* and *B*, respectively, of form (II).

In the refinement of form (II), the data were merged using MERG4 in *SHELXL97* (Sheldrick, 2008), according to the standard procedure for X-ray Mo $K\alpha$ measurements of chemical compounds without heavy atoms. The *E* statistics and *N* (*Z*) test for form (II) confirmed the choice of the noncentrosymmetric space group $P2_1$. The absolute structure was not determined and, while the two independent molecules are an enantiomorphic pair, the choice of absolute configuration for the reference molecules was arbitrary.

For both compounds, data collection: *SMART* (Bruker, 2003); cell refinement: *SAINT* (Bruker, 2003); data reduction: *SAINT*; program(s) used to solve structure: *SHELXS97* (Sheldrick, 2008); program(s) used to refine structure: *SHELXL97* (Sheldrick, 2008); molecular graphics: *ORTEP-3* (Farrugia, 1997) and *Mercury* (Version 2.1; Macrae *et al.*, 2006); software used to prepare material for publication: *SHELXTL* (Version 6.14; Sheldrick, 2008) and *PLATON* (Spek, 2003).

SK is a recipient of a Senior Research Fellowship from CSIR, New Delhi, India. The valuable help provided by Dr Smita Mule in recording the differential scanning calorimetry runs is gratefully acknowledged. This work was supported by the DST, New Delhi, India. We are grateful to Professor C. Glidewell for valuable suggestions and constructive criticism.

Supplementary data for this paper are available from the IUCr electronic archives (Reference: GD3264). Services for accessing these data are described at the back of the journal.

## References

Bruker (2003). *SADABS* (Version 2.05), *SMART* (Version 5.631) and *SAINT* (Version 6.45). Bruker AXS Inc., Madison, Wisconsin, USA.
Cosgrove, S. D., Steele, G., Austin, T. K., Plumb, A. P., Stensland, B., Ferrari, E. & Roberts, K. J. (2005). *J. Pharm. Sci.* **94**, 2403–2415.
Das, D. & Desiraju, G. R. (2006). *CrystEngComm*, **8**, 674–679.
Farrugia, L. J. (1997). *J. Appl. Cryst.* **30**, 565.
Gonnade, R. G., Shashidhar, M. S. & Bhadbhade, M. M. (2008). *CrystEngComm*, **10**, 288–296.
Gonnade, R. G., Shashidhar, M. S., Bhadbhade, M. M. & Sanki, A. K. (2005). *Chem. Commun.* pp. 5870–5872.
Grooff, D., De Villiers, M. M. & Liebenberg, W. (2007). *Thermochim. Acta*, **454**, 33–42.
Ibberson, R. M., Parsons, S., Allan, D. R. & Bell, A. M. T. (2008). *Acta Cryst.* B**64**, 573–582.
Macrae, C. F., Edgington, P. R., McCabe, P., Pidcock, E., Shields, G. P., Taylor, R., Towler, M. & van de Streek, J. (2006). *J. Appl. Cryst.* **39**, 453–457.
Murali, C., Shashidhar, M. S., Gonnade, R. G. & Bhadbhade, M. M. (2007). *Eur. J. Org. Chem.* **7**, 1153–1159.
Parthasarathy, R. & Eisenberg, F. Jr (1986). *Biochem. J.* **235**, 313–322.
Potter, B. V. L. & Lampe, D. (1995). *Angew. Chem. Int. Ed. Engl.* **34**, 1933–1972.
Praveen, T., Samanta, U., Das, T., Shashidhar, M. S. & Chakrabarti, P. (1998). *J. Am. Chem. Soc.* **120**, 3842–3845.
Roy, S., Bhatt, P. M., Nangia, A. & Kruger, G. J. (2007). *Cryst. Growth Des.* **7**, 476–480.
Samanta, U., Puranik, V. G., Chakrabarti, P., Thoniyot, P. & Shashidhar, M. S. (1998). *Acta Cryst.* C**54**, 1289–1291.
Sarmah, M. P., Gonnade, R. G., Shashidhar, M. S. & Bhadbhade, M. M. (2005). *Chem. Eur. J.* **11**, 2103–2110.
Sheldrick, G. M. (2008). *Acta Cryst.* A**64**, 112–122.
Spek, A. L. (2003). *J. Appl. Cryst.* **36**, 7–13.
Steiner, T., Hinrichs, W., Saenger, W. & Gigg, R. (1993). *Acta Cryst.* B**49**, 708–718.
Sureshan, K. M., Shashidhar, M. S., Praveen, T. & Das, T. (2003). *Chem. Rev.* **103**, 4477–4503.
Vega, D., Petragalli, A., Fernandez, D. & Ellena, J. A. (2006). *J. Pharm. Sci.* **95**, 1075–1083.
Wishkerman, S. & Bernstein, J. (2006). *CrystEngComm*, **8**, 245–249.